Available online at www.sciencedirect.com
SCIENCE DIRECT
ELSEVIER
Journal of the European Ceramic Society 26 (2006) 1527–1534
ECERS
www.elsevier.com/locate/jeurceramsoc

The critical size mechanism for the anatase to rutile transformation in TiO_2 and doped-TiO_2

D.J. Reidy, J.D. Holmes, M.A. Morris *

Department of Chemistry, Materials Chemistry, University College Cork, Cork, Ireland

Received 18 January 2005; received in revised form 3 March 2005; accepted 12 March 2005
Available online 23 May 2005

Abstract

A series of titania and doped titania materials have been prepared from sol–gel methods using a titanium isopropoxide precursor. Powder X-ray diffraction (PXRD) and secondary electron microscopy (SEM) have been used to follow the anatase to rutile transformation (ART) phase change in this system. PXRD was used to estimate the relative amounts of each phase and the average particle size at a series of temperatures. Importantly, very careful choice of reaction precursors were made so that a wide range of similar samples could be compared, thus removing effects due to preparation. It was found that doping with Si, Zr, Al and tertiary mixtures of these produced an elevated ART temperature whilst Co, Mn and V had the opposite effect. The most likely explanation for the elevation in the ART temperature is the presence of dopant strain fields, which limit mass transport in the system. Lowering of the ART temperature is probably related to creation defect sites, which provide low energy mass transport routes. It was also found that in the majority of samples, the mechanism for phase change was related to attaining a critical particle size. This was measured at around 450 Å independent of the dopant used. Results are discussed in terms of previous work.

Keywords: TiO_2; Phase transformations; Sol–gel method; Precursors-organic

1. Introduction

Control of the microstructure of titania (in particular, the anatase to rutile phase transition (ART)) is vital to the performance of this material in many applications. These applications include sensors, photocatalysis, pigments and electronics.[1] The phase transition is non-reversible because of the greater thermodynamic stability of the rutile phase.[2] The ART is kinetically defined and the reaction rate determined by parameters such as particle shape/size,[3] purity,[3,4] source effects,[5] atmosphere[6] and reaction conditions.[7] It seems clear that the mechanism for phase transformation is one of nucleation and growth.[8,9] In this way, it might be imagined that the phase transition is dominated by effects such as defect concentration,[10] grain boundary concentration[11] and particle packing.[12] However, following careful work by Zhang and Banfield,[13] it seems clear that a critical size mechanism may also be important in the transformation of nanometre sized particles.[7,14]

Doping of titania with cations can be a useful way to control the phase transition temperature. Shannon and Pask postulated that additives that increase the oxygen vacancy concentration act as promoters of the ART and materials that increase the interstitial defect concentrations inhibit the ART.[15] This simple model has been refined so that the ART temperature is now thought to be lowered by any additives that provide nucleation sites (e.g. by preferential segregation)[16] whilst dopants that are of the same valence, non-reducible and occupy interstitial sites will retard the ART.[17] Authors such as Yang et al. have suggested that dopant reduced particle contact can also retard the ART.[18] Yang and Ferreira[19] have also postulated a simple model based on strain energy considerations that provide an additional energy requirement for phase transformation.[20] In this paper, we use a simple sol–gel method to allow a series of sol–gel preparations of doped titania to be prepared so that insight into a general mechanism for a series of similarly

* Corresponding author. Tel.: +353 21 4903608; fax: +353 21 4274097.
E-mail address: m.morris@ucc.ie (M.A. Morris).

0955-2219/$ – see front matter © 2005 Elsevier Ltd. All rights reserved.
doi:10.1016/j.jeurceramsoc.2005.03.246

prepared materials can be gained. In particular, it was hoped to discover whether a critical particle size mechanism was operative for doped materials and to our knowledge, this has not been examined before. The similarity of the preparation is important as many comparative studies have been based on materials of non-similar preparations. The results can be interpreted as resulting from a combination of a critical size model and mass transport considerations.

2. Experimental

Materials were prepared using a true sol–gel method based on the controlled hydrolysis of titanium(IV) isopropoxide (TIP) employing only catalytic amounts of water. The dopant precursors chosen were: zirconium isopropoxide, aluminium-sec-butoxide, tetraethoxysilane, manganese(II) acetylacetonate, cobalt(II) acetylacetonate and vanadium(III) acetylacetonate. These were chosen because they maintained a good clear gel synthesis and so that the same preparation details could be followed in all cases without any modification. These dopants are also chosen because there is evidence of good solubility (to at least 5%) in titania.[15–20] This was confirmed by examining samples by EDAX for local agglomeration. Zirconia appeared to be the least soluble material investigated and this is discussed in depth below. X-ray fluorescence spectroscopy showed that the target composition was obtained in the calcined materials. Briefly, around 35 ml of TIP was dissolved in 50 ml of butan-1-ol. The required amount of metal precursor was then added and the mixture magnetically stirred for 10 min. Separately, 0.56 ml of ∼36% (w/w) HCl was dissolved in 30 ml of butan-1-ol and mixed for 10 min. The second solution was then added to the first and the whole was stirred for a further 15 min. This solution was then left to stand at room temperature for 4–5 days at which point a clear and transparent glass-like gel was formed. These gels were then dried at 60 °C for 5–7 days. The dried materials were ground to a fine powder and divided into several lots, placed in quartz crucibles and calcined in air for 2 h at 50 °C intervals in the temperature range of 200–1100 °C. C:H:N analysis from a CE440 Elemental Analyzer suggested that all traces of carbon are removed on calcination to temperatures of 350 °C above. DTA data are discussed in detail below confirming this analysis. Dopant concentrations are given as weight percent as metal content.

A Philips X'Pert diffractometer, equipped with a Ni filtered Cu Kα radiation source and accelerator detector was used for powder X-ray diffraction (PXRD) data collection. Each scan used took around 120 s. Incident and reflected Stöller slits of 0.2° were used with a programmable divergent slit to maintain a 10 mm footprint at the sample. Scherrer formulism was used to estimate crystallite sizes. A reference for the instrumental resolution was taken from a titania sample calcined at 1200 °C for 120 h. In all cases, at least three reflections were used and the particle size calculated as the average value. Within experimental error of ±10%, all reflections gave the same values but averaging produced more consistent results. It also indicated that the crystallites were essentially isotropic. The relative weight fractions of anatase (W_A) and rutile (W_R) were calculated using the relative intensity of the anatase (1 0 1) peak (I_A) and the rutile (1 1 0) peak (I_R) and the relationships $W_A = 1/[1 + 0.8I_A/I_R]$ and $W_R = 1/[1 + 1.26I_R/I_A]$ as used by Spurr and Meyers.[21] Physical mixing showed this relationship to be followed on our set-up and this is probably because of the similarity in position of these reflections which limits any instrumental contribution. A JEOL JSM 5510 secondary electron microscope (SEM) operating with a 15 kV accelerating voltage was used for collection of micrographs. Powder samples were blown onto a sample stub with double sided graphitic tape. Particles were sputter coated with gold to avoid charging. Thermal analysis was carried out on a Stanton Redcroft STA 1640 with a heating rate 10 °C min^{-1}.

3. Results and discussion

3.1. One percent doped samples

In the first series of experiments, doped titanias with a 1% (by weight as metals) dopant loading were prepared. These are referred to as, e.g., 1% Zr. For some additives, loadings of this value appear to have dramatic changes of the ART temperature[22] whilst other authors find loadings of this level have little or no effect.[23] In this work, we found that 1% dopant levels had a profound effect on the ART temperature.

Typical PXRD data are provided in Fig. 1 for 1% Al-doped material. Phase assignment is made relative to JCPDS files 84-1286 (anatase) and 87-0920 (rutile). At no temperature or preparation in any of this work did we see any evidence for the formation of the brookite phase even when samples were calcined at 25 °C intervals. This may be because the calcination times may have been too long for this highly metastable phase to be observed. This would also suggest that these dopants do not significantly stabilise this phase. In the data shown in Fig. 1, the conversion from the anatase to rutile phase can be clearly seen in the data at 700 and 900 °C. The narrowing of the reflection peaks through the heating process can also be seen. Also shown in the figure are plots of the XRD derived weight fractions[21] of each phase and the particle sizes (Scherrer formulism) through the heating schedule. Note that Scherrer formulism measures a crystallite size not a true particle size, but since no amorphous particles exist around the ART temperature (see below), the term particle size is used throughout. This can also be seen in comparison of PXRD and SEM derived 'particle sizes'; in general, the crystallite size calculated by the Scherrer method and SEM derived data agree reasonably well. Typical SEM data are shown in Fig. 2. For example, for the 1% V sample calcined at 650 °C, XRD gave the particle size as 720 Å whilst SEM gave around 690 Å. Similarly, for 1% Al sample at 825 °C, the XRD derived size = 454 Å and SEM = 395 Å and for 1% Si at 750 °C, XRD size = 260 Å and SEM size = 225 Å. It should be

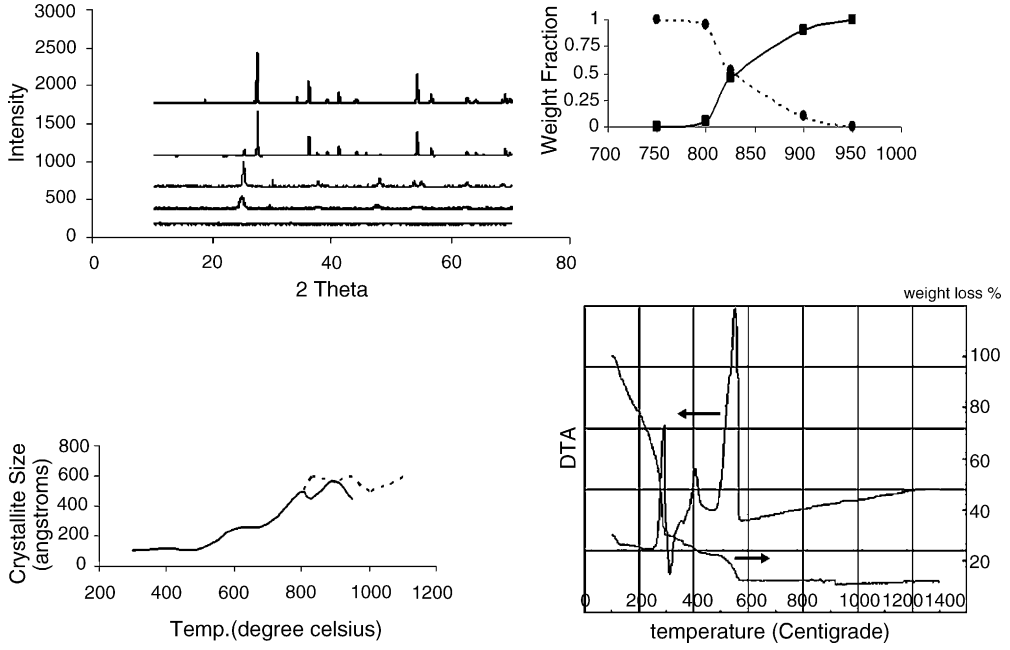

Fig. 1. (A) PXRD data from a 1% Al-doped titania sample. Main figure shows illustrative diffractograms taken at 200, 300, 700, 900 and 1000 °C from bottom to top of the figure respectively. (B) The weight fractions of anatase (- - - -) and rutile (—) against temperature (°C). (C) The particle size (Å) vs. temperature (°C). (D) A typical DTA trace of freshly prepared sample.

pointed out that this correspondence was not true for samples where major particle coalescence was observed as the grains formed were very large, but PXRD profiles were dominated by more local structural effects such as pores, etc. This only affected the samples at the highest calcination temperature of 1100 °C. However, in the temperature range were phase transformation occurred, the SEM derived and XRD derived sizes were in good agreement.

The particle size and weight fraction data can be used to estimate the size of particles at the phase transformation. This size is described as the critical particle size R_c. Since the particle size data represents an average value, taking the R_c value at the onset of the transition probably reflects only the transformation of relatively few nuclei. Instead, the particle size at around 25% of the conversion of anatase to rutile is taken as R_c. Table 1 shows some typical data of particle size versus

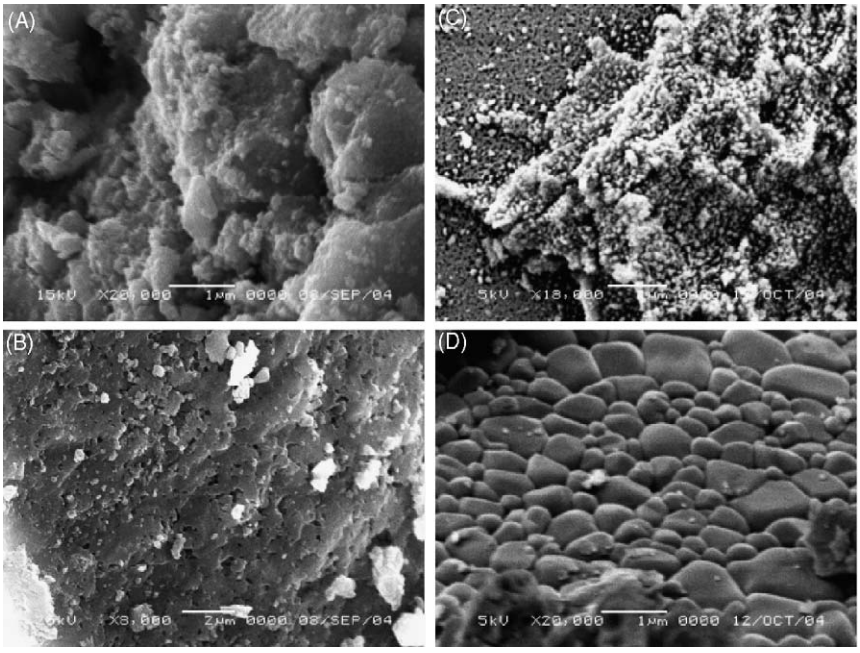

Fig. 2. SEM data from 1% Al at 825 °C (A) and 1100 °C (B) and 1% V at 650 °C (C) and 1100 °C (D). Magnifications as shown in the micrographs.

Table 1
The relationship between the anatase particle size (PS) and the percentage of anatase (%A) in the sample for a few illustrative samples

Sample										
TiO_2	%A	100	100	100	99	77	65	51	10	0
	PS (Å)	122	190	240	375	**451**	270	335	330	330
1% Al	%A	100	100	100	100	99	96	53	42	8
	PS (Å)	130	116	235	305	438	485	**454**	514	563
1% Zr	%A	100	100	100	100	98	68	56	8	
	PS (Å)	113	116	135	230	310	**445**	601	545	
1% V	%A	100	100	100	94	72	6	0		
	PS (Å)	95.2	119	122	369	**461**	928	559		

The value taken as R_c is shown in bold.

temperature as well as the percent anatase present. The estimated R_c value from the data is indicated in the table. Table 2 shows the R_c values for all the 1% doped materials and TiO_2. The R_c values are remarkably consistent (equivalent within experimental error) at around 450 Å (a mean value of 454 Å). The SiO_2 doped data does show some variance and this is partly because between 750 and 850 °C, there is almost no change in the conversion of anatase (around 50% conversion) suggesting two processes are operative at different temperatures. Thus, the particle sizes for each separate conversion were estimated. The higher temperature process appears to be related to the critical particle size seen in the other materials.

At these low dopant levels, there is remarkable consistency in the R_c value even though there is a wide range of phase transition temperatures at around 200 °C. The PXRD data can be used to calculate the phase transition temperature. This was taken as the temperature where 50% of the material was present as anatase (T_{50}) and could be estimated from plots such as the example shown in Fig. 1. Data from each of the samples is shown in Table 3. Together with these data, the temperature where 75% of the anatase phase had been converted to rutile (T_{75}). This additional information allows the 1% Si sample to be compared to the others (because of the well-resolved plateau in the phase transition plot). It can be seen in Table 2 that some of the additives decrease the phase transition temperature whilst others increase the temperature. There is a clear difference between the +4 only oxidation state dopants (which all increase the ART temperature) and the dopants of different or variable valence (which all decrease the ART temperature with the exception of Al^{3+}). The mechanism by which these dopants change the transition can be argued, but it is clear that the role of particle size in the phase change is dominant. Regardless of the incorporation of defect sites, the crucial parameter is reaching the particle size where the thermodynamics of surface rearrangement is balanced by the additional thermodynamic stability of rutile phase compared to the bulk.

Further details of the mechanism for phase change may be gained from consideration of the SEM data. The images shown for vanadium are typical for the low temperature phase changes (i.e. Co, Mn, V and undoped-TiO_2). The lower temperature SEM data of the 1% V (i.e. during phase change) shows that the nanoparticles of anatase and rutile are essentially similar sizes and shape, i.e. no evidence for multiparticle agglomeration prior to phase change (as a mixture of large and small particles might be observed if this agglomeration took place) acting as the driving force for phase transformation was observed. Measurements of particle sizes of rutile and anatase by PXRD also suggested the same thing, i.e. at phase transition, the particle sizes are essentially similar (as in Fig. 1, for example). Data for the other materials (with the exception of silica doping discussed below) are similar and suggests that for all the materials, the particles reach the critical size by a process of 'ripening' where

Table 2
Measured particle size (PS) for each of the 1% doped samples (measured as described in Table 1 together with the measured temperatures for conversion of 50% (T_{50}) and 75% (T_{75}) of anatase for each of the 1% doped samples

Sample	1% Mn	1% Co	1% V	TiO_2	1% Zr	1% Al	1% Si
R_c (Å)	455	463	461	451	445	454	236/448
T_{50} (°C)	640	679	724	751	791	832	787[a]
T_{75} (°C)	651	687	760	782	823	855	863

[a] Not accurately measured because of long plateau in the weight fraction vs. temperature plot around 50% conversion.

Table 3
Measured particle size (PS) and ART temperatures (as T_{50} and T_{75}) for each of the high dopant level samples

Sample	5% Zr	10% Zr	15% Zr	20% Zr	25% Zr	30% Zr	5% ZrAl	5% ZrSi
R_c (Å)	462	446	441	452	312	382	456	277
T_{50} (°C)	830	931	930	924	868	861	844	936
T_{75} (°C)	846	955	963	948	879	932	873	982

smaller particles are consumed by larger particles or by atom diffusion. Fig. 2A shows data from an aluminium-doped sample—showing small nanoparticle agglomerates, but all particles (whether anatase or rutile) are of similar size. We, therefore, conclude that dopants (again with the exception of silica doping) at this concentration do not have significant effect on the influence of grain boundaries or that ground boundary effects do not influence the phase change in these samples.

It should be stated that the ART transition temperatures measured here assume that the phase changes that occur are sequential, i.e. that firstly amorphous material changes to anatase which then changes to rutile and that these phase transformations occur with reasonable temperature separation. This ensures that the PXRD data does represent complete phase change. Differential thermal analysis (DTA) and thermogravimetric analysis (TGA) evidence suggest this is so and typical DTA/TGA data are shown in Fig. 1D. DTA peaks at about 300 and 400 °C are accompanied by large weight losses, and together with residual gas analysis suggest that these are due to solvent loss via desorption and decomposition or reaction. The large DTA peak at 550 °C is accompanied by a 5–10% weight loss (water evolution from inclusions) and is assigned to the exotherm produced by transformation of amorphous TiO_2 to the anatase phase. PXRD data taken below this temperature show no anatase related features whilst data collected above this temperature do indicate the presence of an anatase structure. The anatase to rutile phase transition is at much lower relative intensities and can just be seen at the much higher temperature of around 950 °C. These data also confirm that the materials are free of any adventitious contamination during the anatase to rutile phase transition described in depth herein.

Dopants do effect particle growth beyond the phase change at higher temperatures. Co, Mn, V and undoped-TiO_2, all exhibit the regular grain growth typified by the image in Fig. 2D and such images are consistent with diffusion as the principal growth mechanism rather than particle agglomeration. However, ZrO_2, Al_2O_3 and SiO_2 dopants, all display less regular structures with signs of residual inter- and intra-particle pores from particle agglomeration, but without the formation of well-defined grain boundary structures.

The data here suggest that the dopants control the rate at which particles reach the critical size for phase transformation. In systems of this dopant concentration, it is unlikely that segregation or phase separation occurs and this was not observed here by PXRD. Co, Mn and V might be expected to create anion vacancies to compensate for lower cation charge. These oxygen vacancies are thought to assist phase change by forming nucleation centres.[15,16] It can be concluded that if this anion vacancy model is operative than the particles formed here are of such sizes that any rutile nuclei formed at nucleation centres are not thermodynamically stable and simply convert to anatase before growth can occur. It seems more likely to us that lower transition temperatures are caused by increased mass transport through the vacancy network. The increased ART temperature can be reasonably explained by simple incorporation of the dopant ions and the associated strain fields that reduce mass transport.[19,20] In the next series of experiments, the relevance of this critical size mechanism was tested for high dopant level samples.

3.2. Variable dopant level materials

There was a strong variation in the ART temperature as a function of dopant concentration. This was clearly seen for zirconia-doped samples in the 0–30% range. Typical PXRD data, the derived variation in ART temperature with concentration and a micrograph are shown in Fig. 3. Estimated R_c values (see above) sizes and ART temperatures (as T_{50} and T_{75}) are presented in Table 3. The ART temperature increases to a maximum at 10–15% Zr and then decreases. Importantly, up to the highest loadings of 25 and 30% Zr, the R_c value remains constant at the nominal 450 Å value. This confirms the importance of the critical particle size mechanism at high loadings and at high transformation temperatures. The same critical particle size of ~450 Å is observed for a tertiary doped material 5% Zr, 5% Al (80% Ti). However, a 5% Zr, 5% Si-doped titania exhibited a critical particle size below 300 Å.

The 25 and 30% Zr samples have low R_c values of 312 and 382 Å, respectively. These samples also showed some segregation of a mixed zirconium titanate phase and weak XRD peaks were observed at around 30.5, 33.5, 36, 37.5, 49.5 and 43° 2θ. These are suggestive of the $TiZrO_4$ P212121 orthorhombic phase (JCPDS card number = 07-0290). It may be that the presence of mixed Zr–Ti oxide phases alters the surface or bulk energies, thus, altering the balance of bulk and surface thermodynamics and allowing phase transformation at different critical particle sizes. This follows as the surface free energy of the mixed oxide cannot be expected to be equal to the surface free energy of anatase. All of the zirconia-doped materials at greater than 1% Zr loading do show segregation of ZrO_2 (rather than $TiZrO_4$) at higher temperatures, but this will not alter the surface free energy of the anatase present. This occurs at temperatures above the ART temperature and can be quite clearly seen in the PXRD pattern shown in Fig. 3C where the 29.9° 2θ (1 0 1) reflection of the tetragonal ZrO_2 phase is identified (JCPDS data file 24-1164). The zirconia can be seen in the SEM image in the same figure as very bright particles.

From the data presented here, it was seen that no zirconia segregation or phase separation was observed in anatase and this suggests a high solubility limit as noted by previous workers.[20] There are contrasting views of ZrO_2 solubility in rutile. Authors such as McHale and Roth[24] and Kim et al.[23] suggest high solubility limits whilst Yang and Ferreira[19] show extensive segregation of $ZrTiO_4$ (at high concentrations) and ZrO_2 (low concentrations), and these reports are in good agreement with our findings. The data presented here suggests a maximum solubility of zirconia in rutile of between only 1 and 5% Zr. This was confirmed by taking a (precalcined at 1100 °C for 24 h) 5 wt.% (as metals) ZrO_2 mixture

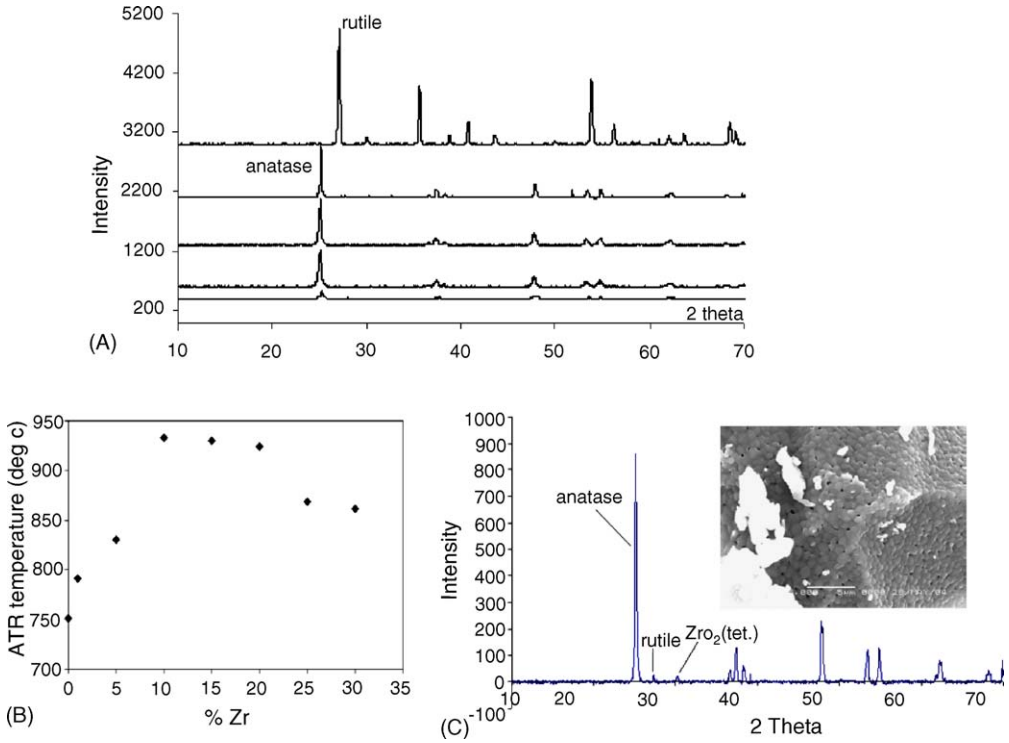

Fig. 3. Typical data for higher loading samples, in this case a 10% Zr sample. (A) Representative PXRD data taken from 300 to 1100 °C (at 200 °C intervals from top to bottom). (B) The variation of ART temperature as a function of percent Zr loading and (C) A detailed diffractogram and (inset) SEM image at 1100 °C.

(in 95 mol% rutile) and calcining at 1100 °C for 366 h. The samples were removed several times during calcination and ground, PXRD data collected and replaced in the oven. No change in the ZrO_2 to TiO_2 peak height ratio was observed confirming very limited or no solubility in this concentration range. However, it is emphasised that the segregation of ZrO_2 during heating of samples in the 10–20% Zr content range does not affect the critical particle size in the same way as $ZrTiO_4$ does.

The mixed Zr–Si-doped material shows no evidence for segregation of any kind by PXRD or by SEM, and this is consistent with previous work.[23] However, the low R_c values measured for these systems might suggest quite different behaviour. SEM micrographs of the 1% Si and the 5% Zr, 5% Si materials might suggest that a mechanism is operative based on particle agglomeration to reach the required particle size. The SEM data were collected following 1000 °C calcinations, i.e. just above T_{50} and is quite unlike that from any other samples. All of the other non-silica-doped samples exhibited significant combinations intra- and inter-particle macroporosity. The well-developed macro-pore structure was absent from SEM images of silica containing materials which appeared non-porous at these magnifications (although the samples do show some very limited mesoporosity by TEM and adsorption isotherms). The data suggest that particle agglomeration does occur for silica-based samples. This is confirmed when particle size versus calcination temperature plots are drawn (Fig. 4C and D) where it can be clearly seen that at the transition temperature, the rutile particle size is much greater than that of anatase suggesting phase transition is commensurate with a rapid growth of particles.

3.3. Closing remarks

Other authors have discussed the possibility of a critical particle size mechanism for the transformation of anatase to rutile.[8,13,14] The R_c values measured by these authors are somewhat smaller than here being 130–150 Å. The difference in R_c values may be attributable to the differing preparative routes as the previous authors carried out preparation in high concentration of water compared to here where only catalytic amounts of water are used and a true alkoxide continuous sol–gel phase is prepared compared to a more colloidal product. There is no fundamental reason to believe that there will be a unique R_c for TiO_2 as different preparations will provide morphologically different particles and phase development and growth is closely related to particle shape and size.[25] One can also expect differences due to defect densities and pore structure. However, the work presented here shows that a critical particle size is central to the transformation of anatase to rutile for both pure and doped materials and to our knowledge, this is the first time that the role of a critical particle size has been demonstrated for a range of dopants over a wide range of concentrations.

A critical particle size mechanism for anatase to rutile transformation occurs because the surface free energy of

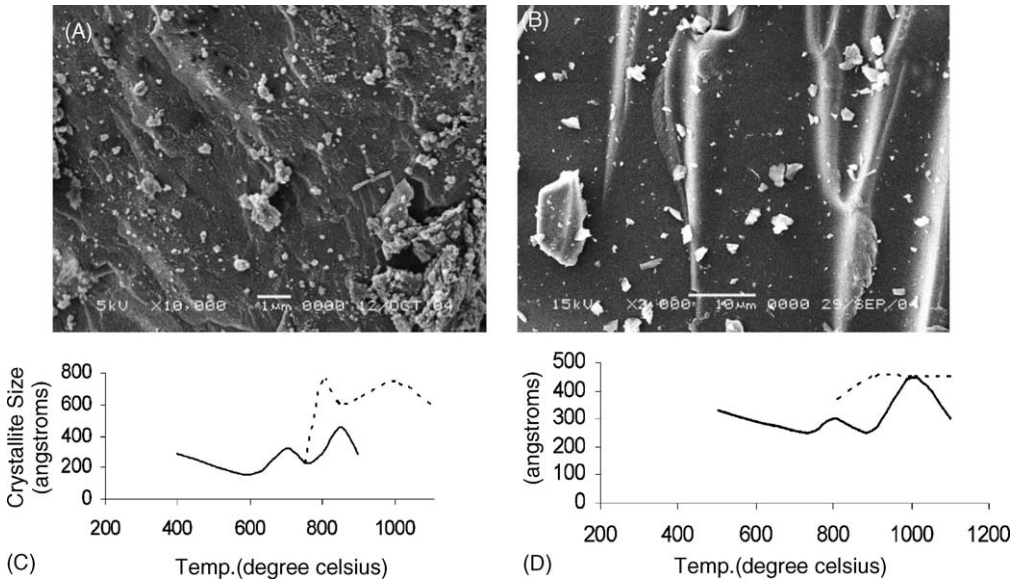

Fig. 4. SEM images recorded at 1000 °C of 1% Si (A) and 5%, Zr 5% Si (B) materials together with the plots of particle size vs. calcination temperature (C) and (D), respectively. In (C) and (D), the solid line represents anatase data and the dashed line rutile data.

anatase is lower than that of rutile—the reverse of the bulk situation.[26] An R_c value of 450 Å was measured here and, of the materials prepared, only those containing silica dopants and very high zirconia loadings showed an experimentally significant variation from this. It was thought that the formation of $ZrTiO_4$ phases might have altered the surface energetics allowing smaller particle phase transformation. In the case of silica doping, it was seen that this dopant very effectively promotes particle agglomeration so that particles below the expected R_c value merge and 'spontaneously', within the timeframe of the calcination treatment, transform into rutile.

The surprising feature of this work is just how insensitive to doping (concentration, type) this critical particle size mechanism is. The same R_c value was observed for systems which introduce non-stoichiometric defects in the system and even in systems where phase separation was known and demonstrated to occur. It might be expected that phase separation and defect formation would increase the rate of phase change nucleation. For the small particles prepared here, nucleation appears not to be the rate-limiting step in phase transformation. Instead, the rate-limiting step appears to be related to the mass transport requirements of reaching the critical particle size. We would suggest that dopants affect the transformation process by increasing or decreasing the rate of mass transport. This is a true nanoscale property as for larger anatase particles nucleation might be the rate limiting.

Acknowledgements

The authors would like to thank the Enterprise Ireland Basic Research Grant Scheme and the HEA (Ireland) PRTL II Scheme for student support. R. Farrell is thanked for SEM assistance.

References

1. Vogel, R., Hoyer, P. and Weller, H., *J. Phys. Chem.*, 1994, **98**, 3183; Liu, D. and Kamat, P. V., *J. Electroanal. Chem. Interfacial Electrochem.*, 1993, 451; Sukharev, V. and Kershaw, R., *J. Photochem. Photobiol. A: Chem.*, 1996, **98**, 165; Al-Salim, N. I., Bagshaw, S. A., Bittar, A., Kemmitt, T., McQuillan, A. J., Mills, A. M. *et al.*, *J. Mater. Chem.*, 2000, **10**, 2358.
2. Rao, C. N. R. and Rao, K. J., *Phase Transitions in Solids*. McGraw-Hill, New York, 1978 (Chapter 2).
3. Yoganarasimhan, S. R. and Rao, C. N. R., *Trans. Faraday Soc.*, 1962, **58**, 1579.
4. MacKenzie, K. J. D., *Trans. J. Br. Ceram. Soc.*, 1975, **74**, 29.
5. Byun, C., Wang, J. W., Kim, L. T., Hong, K. S. and Lee, B. W., *Mater. Res. Bull.*, 1997, **32**, 431.
6. MacKenzie, K. J. D., *Trans. J. Br. Ceram. Soc.*, 1975, **74**, 121.
7. Li, Y., White, T. J. and Lim, S. H., *J. Sol. State Chem.*, 2004, **177**, 1372.
8. Gribb, A. A. and Banfield, J. F., *Am. Miner.*, 1977, **82**, 717.
9. Ding, X.-Z. and Liu, X.-H., *J. Mater. Res.*, 1998, **13**, 2556.
10. Zhang, H. and Banfield, J. F., *J. Mater. Res.*, 2000, **15**, 437.
11. Ahn, Y. U., Kim, E. J., Kim, H. T. and Hahn, S. H., *Mater. Letts.*, 2003, **57**, 4660.
12. Kumar, K. P., Keizer, K., Burggraaf, A. J., Okubo, T. and Nagamoto, H., *J. Mater. Chem.*, 1993, **3**, 1151.
13. Zhang, H. and Banfield, J. F., *J. Phys. Chem.*, 2000, **B104**, 3481.
14. Hu, Y., Tsai, H.-L. and Huang, C.-L., *Mater. Sci. Eng.*, 2003, **A344**, 209.
15. Shannon, R. D. and Pask, J. A., *J. Am. Ceram. Soc.*, 1965, **48**, 391.
16. Chao, H. E., Yan, Y. U., Xingfang, H. U. and Larbol, A., *J. Eur. Ceram. Soc.*, 2003, **23**, 1457, and references therein.
17. Arroya, R., Corgoba, G., Padilla, J. and Lara, V. H., *Mater. Letts.*, 2002, **54**, 397.

18. Yoshinaka, M., Hirota, K. and Yamaguchi, O., *J. Am. Ceram. Soc.*, 1997, **80**, 2749.
19. Yang, J. and Ferreira, J. M. F., *Mater. Res. Letts.*, 1998, **33**, 389.
20. Kingery, W. D., Bowen, H. K. and Uhlmann, D. R., *Introduction to Ceramics* (*2nd ed.*). Wiley & Sons, New York, 1976, p. 58,431.
21. Spurr, R. A. and Myers, H., *Anal. Chem.*, 1957, **29**, 760.
22. Janes, R., Knoightley, L. J. and Harding, C. J., *Dyes Pigments*, 2004, **62**, 199.
23. Kim, J., Song, K. C., Foncillas, S. and Pratsinis, S. E., *J. Eur. Ceram. Soc.*, 2001, **21**, 2863.
24. McHale, A. E. and Roth, R. S., *J. Am. Ceram. Soc.*, 1986, **69**, 827.
25. Penn, R. L. and Banfield, J. F., *Geochim. Cosmochim. Acta*, 1999, **63**, 1549.
26. Zhang, H. and Banfield, J. F., *J. Mater. Chem.*, 1998, **8**, 2073.